Conservative Estimation of Whole-Body Averaged SAR in Infants with Homogeneous and Simple-Shaped Phantom in GHz Region

Akimasa Hirata, Naoki Ito, Osamu Fujiwara, Tomoaki Nagaoka*, and Soichi Watanabe*
Department of Computer Science and Engineering, Nagoya Institute of Technology, Japan
E-mail: ahirata@nitech.ac.jp, fujiwara@odin.nitech.ac.jp
*National Institute of Information and Communications Technolgoy, Japan
E-mail: nagaoka@nict.go.jp, wata@nict.go.jp

Abstract

We calculated the whole-body-averaged specific absorption rates (WBSARs) in a Japanese nine-month-old infant model and its corresponding homogeneous spheroidal and ellipsoidal models with 2/3 muscle tissue for 1-6 GHz far-field exposure. As a result, we found that in comparison with the WBSAR in the infant model, the ellipsoidal model with the same frontally-projected area as that of the infant model, provides an underestimate, whereas the ellipsoidal model with the same surface area yields an overestimate. In addition, the WBSARs in the homogenous infant models were found to be strongly affected by the electrical constant of tissue, and to be larger in the order of 2/3 muscle, skin and muscle tissues, regardless of the model shapes or polarization of incident waves. These findings suggest that the ellipsoidal model having the same surface area as that of the infant model and electrical constants of muscle tissue provides a conservative WBSAR over wide frequency bands. To confirm this idea, based on the Kaup index for Japanese nine-month-old infants, which is often used to represent the obesity of infants, we developed linearly-reduced nine-month-old infant models and the corresponding muscle-ellipsoidals, and re-calculated their whole-body average SARs with respect to body shapes. Our results reveal that the ellipsoidal model with the same surface area as that of a nine-month-old infant model gives a conservative WBSAR for different infant models, whose variability due to the model shape reaches 15%.

Keywords: whole-body exposure, nine-month-old infant model, whole-body average SAR, conservative estimation

1. Introduction

There has been increasing public concern about the adverse health effects of human exposure to electromagnetic (EM) waves. According to the safety guidelines of the ICNIRP (International Commission on Non-Ionizing Radiation Protection) [1998] and the IEEE standard [2006], the whole-body averaged specific-absorption-rate (WBSAR) is used as a metric of basic restriction for radio frequency (RF) whole-body exposures. The basic restriction of WBSAR is 0.4 W/kg for occupational exposure or 0.08 W/kg for public exposure. An incident electric /magnetic field, which does not produce EM absorption exceeding the above limit is defined as a reference level in the ICNIRP guidelines [1998] and as the maximum permissible exposure in the IEEE standard [2006]. The relationship between the reference level/maximum permissible exposure and the WBSAR was derived mainly from numerical calculations done dozens of years ago.

In computational dosimetry in the 1980s, human modeling was highly simplified in the figure of a prolate spheroid or a homogeneous block model [Durney, 1980; Gandhi, 1980]. In recent years, with the development of computational resources, anatomically based human body models are used for investigating the WBSAR [Dimbylow 2002, Sandini 2003, Nagaoka et al 2004, Dimbylow 2005, Wang et al 2006, Hirata et al 2007a, Dimbylow and Bolch 2007, Conil et al 2008]. As the main result, the WBSAR under the reference level/ maximum permissible exposure is found to have a peak around several dozen megahertz due to standing waves over the body model. In addition, the WBSAR has another peak around 2 GHz, which is caused by a relaxation of the reference level/maximum permissible exposure with an increase in the frequency (e.g., Dimbylow 2002, Sandini et al 2003, Wang et al 2006, Conil et al 2008). Furthermore, the WBSARs in the child models were larger than those in the adult (Dimbylow 2002, Wang et al 2006, Dimbylow and Bloch 2007, Conil et al 2008). Recently, Dimbylow and Bloch (2007) investigated the WBSAR in a realistic nine-month-old infant model for frequencies up to 6 GHz, which demonstrated that the WBSAR in the nine-month-old child model is further larger than that in a four-year-old child model in the GHz region.

In the standards/guidelines, homogeneous and simple-shaped models have been used in order to determine the reference level/maximum permissible exposure against the basic restriction of WBSAR. However, it is not clear that the WBSAR in the homogeneous and simple-shaped models could give a conservative estimate compared to that in anatomically-based human models. In addition, such simplified models in great demand for discussing the variability of the WBSA, since it is difficult to develop new numeric human models of different heights and weights due to the large expenditure of funds and the time involved. In the present study, we investigated the WBSARs in a Japanese nine-month-old infant model and its corresponding homogeneous and simple-shaped models (i.e., spheroidal and ellipsoidal). Based on the results obtained, we propose a homogeneous and simple-shaped model which could give a conservative

estimation compared to an anatomically-based human model.

2. Model and Methods

A. Computational Methods

The Finite-Difference Time-Domain (FDTD) method (Taflove and Hagness 2005) is used for computational dosimetry. Either one of human models is located in free space. As a wave source, a plane wave with both vertical polarization (VP) and the horizontal polarization (HP) were considered. A 24-layered uniaxial-Perfectly Matched Layer was used as the absorbing boundary. The separation between the model and the absorbing boundary was set at 100 cells. The electrical constants of tissues were taken from a report by Gabriel (1996).

B. Numeric Human Phantoms

Nine-month infant Phantoms: Dimbylow and Bloch (2007) reported that the WBSAR in a nine-month-old infant is larger than that in a three-year-old child model. Thus, we developed a nine-month-old infant model by linearly reducing a three-year-old Japanese child model (Nagaoka *et al* 2008), which was developed by applying a free-form deformation algorithm to the Japanese adult male model (Nagaoka *et al* 2004). In developing the three-year-old child model, a total of 66 body dimensions was taken into account for reducing each part, and manual editing was applied in order to maintain anatomical validity. The resolution of these models was 2 mm segmented into 51 anatomic regions. The height and weight of the three-year-old child model developed in the present study were 0.90 m and 13.0 kg, respectively. The chosen height and weight of the nine-month-old child model were 0.70 m and 8.9 kg, respectively, so as to coincide with the average values for Japanese infants. The resolution of the model is 1 mm, which is the resolution required for computational simulation with the FDTD method up to 6 GHz. The disadvantage of the nine-month infant model is that the body shape and anatomical correctness may not be fully maintained, since we simply reduced it from the three-year-old child model. The schematic view of the nine-month-old infant model is illustrated in figure 1, together with simplified phantom given below.

Simple-shaped Phantom: For fundamental discussion on WBSAR, we considered spheroidal and ellipsoidal models corresponding to the above nine-month-old infant (see figure 1). The parameters of the spheroid were chosen so that its height and weight coincided with those of the infant model. We defined two ellipsoids (A and B) in terms of their eccentricity (circle: 0, parabola: 1), while their height and weight were identical to those of the infant model. The eccentricity of ellipsoid A was determined so that the frontally-projected area matched as that of the infant model, while that of ellipsoid B was determined based on the model surface area. The parameters of the models considered in the present studies are listed in Table 1.

Three-Layered Ellipsoids: In order to discuss the model inhomogeneity, we considered

three-layered ellilpsoids. In the following section, we will choose ellipsoid B as an example for this investigation. The outer layer of that model is skin with the thickness of a single cell, and the next layer is fat with variable thickness, and the remainder is muscle (see figure 1).

Nine-month Infant Phantoms for Discussing the Variability of the WBSAR: In order to discuss the variability of the WBSAR in infants, we developed additional Japanese nine-month-old infant models based on the Kaup index, which is often used to represent the obesity of infants instead of the body mass index (BMI) used for adults (Zannolli and Morgese 1996, Komiyama et al 2004). These indices are essentially the same except for the unit and significant figures. The Kaup index is defined as the weight [g] divided by the square of the height [cm^2] multiplied by a factor of 10. Based on the data provided by the Research Institute of Human Engineering for Quality Life (2006), we calculated the Kaup index and its standard deviation for Japanese infants. Note that both the Kaup index and the BMI follow the normal distribution (Zannolli and Morgese 1996). Our attention was focused on the infant for two standard deviations of the mean value. Assuming that the height of the infant is fixed at 0.70 m, we determined the corresponding linearly-reduced realistic models with different Kaup indices. The mean value of the nine-month-old child was 17.7 and its standard deviation was 1.5. We then calculated the parameters of these models so that the minimum and maximum Kaup indices emerged as 15 and 21, respectively. The parameters of the models developed are listed in Table 2.

3. Computational Results

A. Fundamental Investigation of WBSAR in Different Human Body Models

First, let us discuss the effect of model shape on the WBSAR. The WBSAR in the nine-month-old child model and its corresponding ellipsoidal/spheroidal models is plotted in figure 2 for VP and HP. In order to investigate the effect of model inhomogeneity, a homogeneous anthropomorphic model comprised of 2/3 muscle was also considered. As seen from figure 2, the spheroidal model and ellipsoidal model A gave an underestimation of WBSAR compared to the infant model over the frequency region considered, while the ellipsoidal model B gave an overestimation. For the ellipsoidal model B, the WBSARs for exposure with VP and HP are comparable, since the electromagnetic absorption in the GHz region is concentrated around the model surface. The feature of ellipsoidal model B is its small depth or large eccentricity, as shown in Table 1. The tendency in fig. 2 was shown in the Japanese three-year-old child model, to which manual editing was conducted to keep the anatomical reliability.

Next, we considered three-layered ellipsoid models in order to discuss the effect of model inhomogeneity on the WBSAR. Fig. 3 shows the frequency dependency of WBSAR in the

three-layered ellipsoidal models, together with anatomically based infant models. The WBSAR calculated for the model developed at the University of Florida (Dimbylow and Bolch, 2007) is also shown for comparison. As seen from fig. 3, the WBSAR in different models show peaks at different frequencies. Such peaks in the WBSAR of an anatomically-based model were observed to be around 2-3 GHz, but much smaller than those of layered ellipsoidal models.

Furthermore, Fig. 4 shows the WBSAR in the models whose electrical constants are those of 2/3 muscle, skin, and muscle, which indicates the effect of electrical constants of the tissue on the WBSAR. The respective results for VP and HP are plotted in fig. 4 (a) and (b). From fig. 4(a), the WBSARs in the models with skin and muscle are 5% and 12-15% smaller, respectively, than that for 2/3 muscle, independent of the model shape. This tendency is identical to exposure with HP, as seen from fig. 4(b), suggesting that the ellipsoid B whose electrical constants were chosen as those of muscle provides a conservative WBSAR. The same tendency was observed for the three-year-old child model, although it is not shown here for avoiding repetition (Nagaya et al 2007).

B. Variability of WBSAR in Nine-Month-Old Infant Models

Fig. 5 shows the frequency characteristics of the WBSAR for infant models with different Kaup indexes and their conservative models proposed in the above subsection. Note that those for the three-year-old model is also plotted in order to confirm our idea. The effectiveness of the conservative models proposed in the present study is confirmed from this figure, which also reveals that the variability of the WBSAR due to the model shape reaches ±15%. The WBSAR increased for infant models with a smaller Kaup index or lower weight. The effectiveness of the conservative model was confirmed for the three-year-old model whose anatomical construction is more reliable than those in the nine-month-infant models.

4. Discussions

In Sec. 3. A, we confirmed that the dominant factor influencing the WBSAR in the GHz region is the model surface area, but neither can the effect of electrical constants and the inhomogeneity of tissues be neglected, as suggested by Hirata et al (2007a). According to Hirata et al (2007b) and Nagaya et al (2008), the absorption cross section is almost proportional to the model surface area for models with similar anatomical structure, although the slope of its regression line depends on the model shape. As can be seen in fig. 2, on the other hand, the WBSAR in ellipsoidal model B, whose surfaced area is the same as that of the nine-month infant model, is larger than that of the nine-month infant model by 30% or more.

A significant peak seen in fig. 3 was observed in the three-layered or idealized phantom, whereas such a peak appeared around 2-3 GHz and is unclear in the anatomically based human

models; not only for the one developed in the present study but also for the model developed at the University of Florida (Dimbylow and Bolch 2007). These results suggest that clear peaks of the WBSAR in the layered model would not appear in the anatomically based model, due to the variability of the thickness of its skin and fat.

From fig.4, the WBSAR in homogeneous ellipsoidal model B is large on the order of 2/3 muscle, skin and muscle, regardless of incidental electromagnetic polarization, which means that the WBSAR can be adjustable by choosing the proper electrical constants over wideband frequency regions. The above consideration implies that the muscle-ellipsoidal model, whose surface area is the same as that of the infant model could yield conservative estimations of WBSAR compared to the anatomically-based model in frequencies from 1 GHz to 6 GHz. The main reason for the higher WBSAR in the model with lower conductivity has been attributed to the reflection coefficient at the air-model boundary or impedance matching (Rowlandson and Barber 1979, Dimbylow 2005). One of the concerns of the conservative model defined in the present study is that the WBSAR in the conservative and realistic models approached around 3 GHz, and then the WBSAR in both the anatomically based model decreased by more than 3 GHz. This tendency of the anatomically based model cannot be realized using a homogeneous ellipsoidal model. The main factor influencing the tendency is the model's inhomogeneity, as seen from fig. 3. The reason for the enhancement of electromagnetic absorption may be due to standing waves (see Dorossos et al 2000 for a one-dimensional model). Note that Drossos et al (2000) defined the conservative electrical constants of a one-dimensional multi-layered model for *localized exposures*, especially for handset antennas, while the variability of tissue thickness over the whole body is much greater than that for the head alone.

Infants generally have a thin fat layer that may not be represented in the reduced infant models. For a model with a thin fat layer, however, it would result in a lower WBSAR due to impedance matching at the air-body boundary (Dimbylow 2005). The WBSAR in actual infants with a Kaup index of 15 would, therefore, be somewhat lower than those of the corresponding linearly-reduced infant model (see fig. 5).

5. Conclusions

We calculated the WBSAR in a nine-month-old infant model and its corresponding spheroidal and ellipsoidal models for 1-6 GHz far-field exposure. Using these models, we investigated the effects of i) model shapes, ii) electrical constants of tissue, and iii) model inhomogeneity on the WBSAR. From our computational results, we proposed a homogeneous ellipsoid which yields an overestimate of the WBSAR in the following way. The electrical constants of the ellipsoid were chosen as those of muscle so as to give a conservative estimation over the frequency region considered.

In order to confirm the effectiveness of the conservative model proposed in the present study, we developed linearly-reduced nine-month-old infant models and their corresponding muscle-ellipsoidals based on the Kaup index for Japanese nine-month-old infants. Our results reveal that the ellipsoid with the same surface area as that of a nine-month-old infant model yielded a conservative WBSAR, whose variability in nine-month-old infants reaches 15%.

Future work is to validate our conservative model for actual infant models.

Acknowledgements

This work was supported in part by Grant-in-Aid for Scientific Research (B), and a Research Grant from Telecom Engineering Center, Japan.

REFERENCES

Conil E, Hadjem A, Lacroux F, Wong M F, and Wiart J 2008 Variability analysis of SAR from 20 MHz to 2.4 GHz for different adult and child models using finite-difference time-domain *Phys. Med. Biol.* **53** 1511-1525

Dimbylow P J 2002 Fine resolution calculations of SAR in the human body for frequencies up to 3 GHz *Phys. Med. Biol.* **47** 2835-2846

Dimbylow P J 2005 Resonance behavior of whole-body averaged specific energy absorption rate (SAR) in the female voxel model, NAOMI **50** 4053-4063

Dimbylow P and Bolch W 2007 Whole-body-averaged SAR from 50 MHz to 4 GHz in the University of Florida child voxel phantoms *Phys. Med. Biol.* **52** 6639-6649

Nagaoka T, Watanabe S, Sakurai K, Kunieda E, Watanabe S, Taki M, and Yamanaka Y 2004 Development of realistic high-resolution whole-body voxel models of Japanese adult males and females of average height and weight, and application of models to radio-frequency electromagnetic-field dosimetry *Phys. Med. Biol.* **49** 1-15

Nagaoka T, Kunieda E, and Watanabe S 2008 Proportion-corrected scaled voxel models for Japanese children and their application to the numerical dosimetry of specific absorption rate for frequencies from 30 MHz to 3 GHz *Phys Med Biol* (accepted)

Hirata A, Kodera S, Wang J and Fujiwara O 2007a Dominant factors influencing whole-body average SAR due to far-field exposure in whole-body resonance frequency and GHz regions *Bioelectromagnetics* **28** 484-487

Hirata A, Nagaya Y, Fujiwara O, Nagaoka T, and Watanabe S 2007b, A formula for predicting whole-body average SAR in human models for far-field exposure at GHz bands *Proc. Bioelectromagnetics Annual Meeting*, 2-6

International Commission on Non-Ionizing Radiation Protection (ICNIRP) 1998 Guidelines for limiting exposure to time-varying electric, magnetic, and electromagnetic fields (up to 300 GHz) *Health Phys.* **74** 494-522

Komiyama S, Masuda T, Nakao T, and Teramoto K 2004 The relationships between stature, fat-free mass index, and fat mass index at before and after BMI-rebound in children *J. Health Sci.* **26** 31-39

Nagaya Y, Hirata A, Fujiwara O, Nagaoka T, and Watanabe S 2007 Conservative prediction of

whole-body average SAR in infant model of 0.3-6GHz far field exposure *Tech Rep IEICE* EMCJ2007-102

Nagaya Y, Hirata A, Fujiwara O, Nagaoka T, and Watanabe S 2008 A formula and uncertainty of GHz-band whole-body average SAR based on the correlation between absorption cross section and body surface area of human *IEICE Trans.* **J91-B** 199-206

Penman A D and Johnson W D 2006 The changing shape of the body mass index distribution curve in the population: implications for public health policy to reduce the prevalence of adult obesity *Prev. Chronic Dis.* **3** A74

Research Institute of Human Engineering for Quality Life 2006 Body size database of Children 2005-2006 (http://www.hql.jp/database/index.html)

Sandrini L, Vaccari A, Malacarne C, Cristoforetti L and Pontalti 2004 RF dosimetry: comparison between power absorption of female and male numerical models from 0.1 to 4 GHz *Phys Med Biol.* **49** 5185-5201

Taflove A and Hagness S 2003 Computational Electrodynamics: The Finite-Difference Time-Domain Method: 3rd Ed. Norwood, MA: Artech House

Wang J, Fujiwara O, Kodera S, Watanabe S 2006 FDTD calculation of whole-body average SAR in adult and child models for frequencies from 30 MHz to 3 GHz *Phys. Med. Biol.* **51** 4119-4127.

Zannolli R and Morgese G 1996 Distribution of BMI in children: prevalence of wasting and fattening conditions *Ann. Hum. Biol.* **23** 63-69

FIGURE AND TABLE CAPTIONS

Figure 1. (a) Three-year-old child and (b) nine-month-old infant models. The latter was developed by linearly reducing the former. (c) Spheroidal and (d) ellipsoidal models corresponding to the nine-month-old infant model.

Figure 2. Frequency characteristics of WBSARs for different body models (power density of incident wave was 10 W/m^2).

Figure 3. WBSAR in three-layered ellipsoidal models (power density of incident wave was 10 W/m^2).

Figure 4. Dependency of WBSAR on electrical constants of tissue for (a) VP and (b) HP (power density of incident wave was 10 W/m^2).

Figure 5. WBSARs in nine-month-old infant and its corresponding conservative models with different Kaup indexes (power density of incident wave was 10 W/m^2).

Table 1. Parameters of nine-month infant model and its corresponding simple-shaped models.

Table 2. Parameters of nine-month infant and its conservative models.

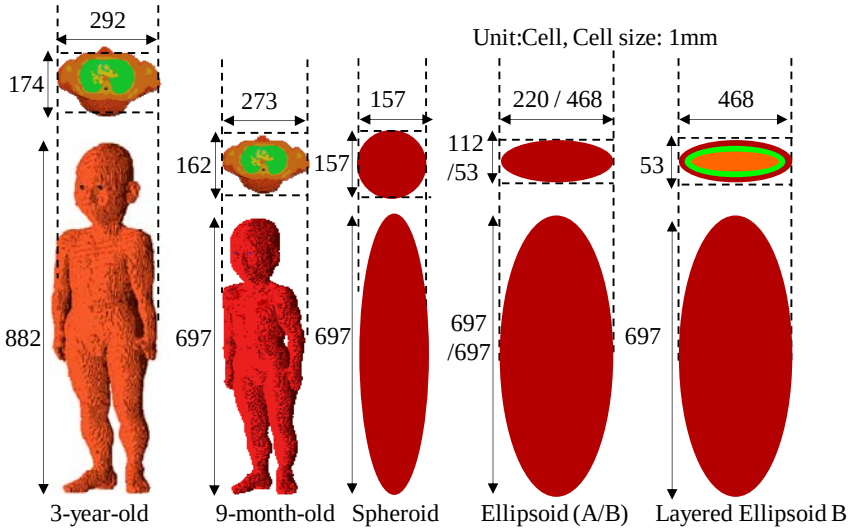
Unit:Cell, Cell size: 1mm
292
174
882
273
162
697
157
157
697
220 / 468
112
/53
697
/697
468
53
697
3-year-old
9-month-old
Spheroid
Ellipsoid (A/B)
Layered Ellipsoid B

Fig. 1

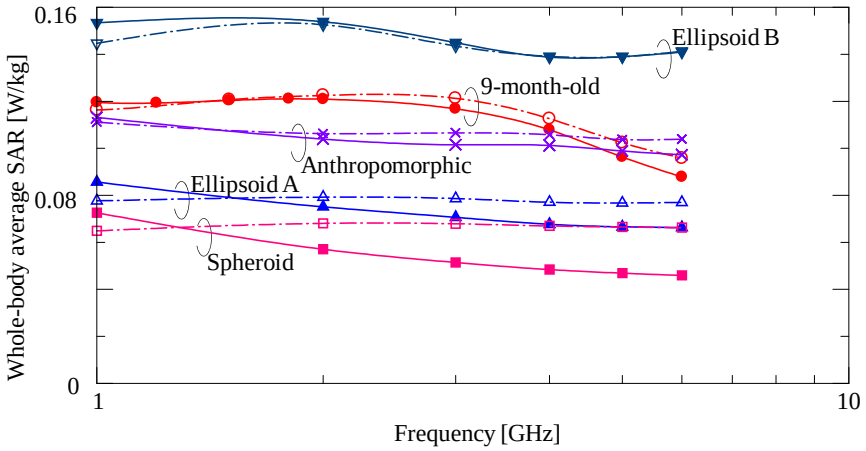
0.16
0.08
0
1
10
Whole-body average SAR [W/kg]
Frequency [GHz]
Ellipsoid B
9-month-old
Anthropomorphic
Ellipsoid A
Spheroid

Fig. 2

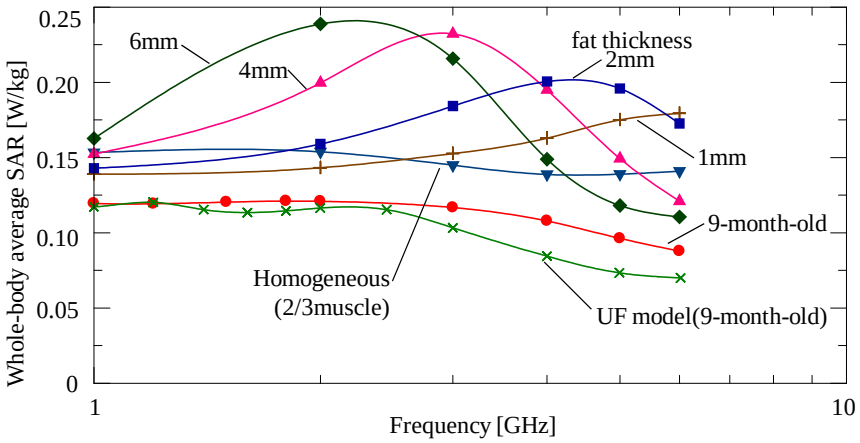
0.25
0.20
0.15
0.10
0.05
0
Whole-body average SAR [W/kg]
1
10
Frequency [GHz]
6mm
4mm
fat thickness
2mm
1mm
9-month-old
Homogeneous
(2/3muscle)
UF model(9-month-old)

Fig. 3

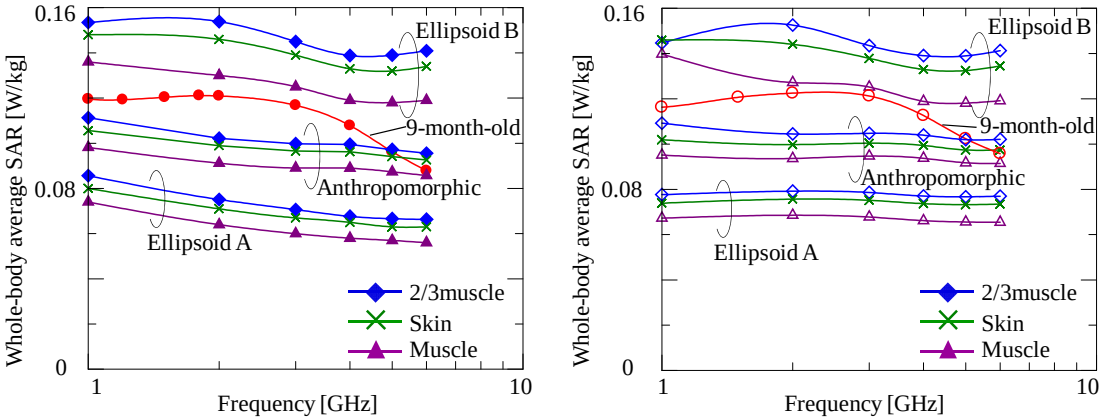
0.16
0.08
0
Whole-body average SAR [W/kg]
1
10
Frequency [GHz]
Ellipsoid B
9-month-old
Anthropomorphic
Ellipsoid A
2/3muscle
Skin
Muscle
(a)
(b)

Fig. 4

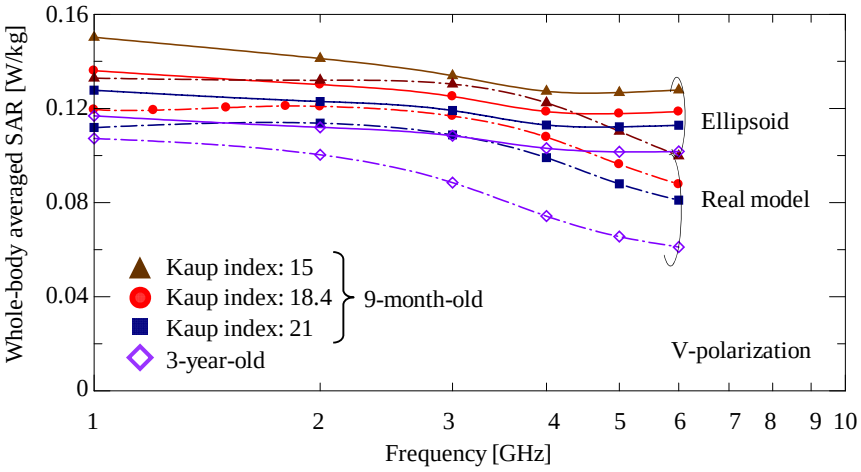
0.16
0.12
0.08
0.04
0
Whole-body averaged SAR [W/kg]
1
2
3
4
5
6
7
8
9
10
Frequency [GHz]
Ellipsoid
Real model
Kaup index: 15
Kaup index: 18.4
Kaup index: 21
9-month-old
3-year-old
V-polarization

Fig. 5

	Anthropomorphic	Spheroid	Ellipsoid	
			A	B
Height[m]	0.7	0.7	0.7	0.7
Weight[kg]	8.95	8.95	8.95	8.95
Eccentricity	-	0	0.86	0.99
$S_M[m^2]$	0.60	0.38	0.40	0.60
$S_F[m^2]$	0.12	0.09	0.12	0.26

S_M : Model surface area S_F : Frontally-projected area

Table 1

	Anthropomorphic			Ellipsoid B		
	15	18.4	21	15	18.4	21
Height[m]	0.7	0.7	0.7	0.7	0.7	0.7
Weight[kg]	7.29	8.95	10.2	7.30	8.95	10.3
Kaup index	15	18.4	21	15	18.4	21
$S_M[m^2]$	0.53	0.60	0.66	0.53	0.60	0.66
$S_F[m^2]$	0.11	0.12	0.13	0.22	0.26	0.28

S_M : Model surface area S_F : Frontally-projected area

Table 2